JMEPEG (2012) 21:2657–2662
DOI: 10.1007/s11665-012-0285-1

1059-9495/$19.00

A Methodology for the Development, Production, and Validation of R-Phase Actuators

K. Lygin, S. Langbein, P. Labenda, and T. Sadek

(Submitted February 20, 2012; in revised form May 30, 2012)

The R-phase transformation has interesting features with potential for applications that need a small temperature hysteresis and good dynamic behavior, such as thermostatic valves. The aim of this article is to show the development, production, and validation process of different R-phase shape memory alloy (SMA) actuators, starting with a semi-finished wire and concluding with a finalized R-phase spring actuator. This study focuses mainly on the calculation, the thermomechanical treatment, and experimental validation of the designed actuators. The first section of this article presents a mathematical dimensioning tool for different R-phase actuators, especially for extension SMA springs. The second part shows specific parameters on the R-phase transformation during thermomechanical treatment. The parameters Ni-content and annealing temperature are being varied to achieve different transformation behavior of the R-phase. The third section relates to the production process of calculated SMA spring actuators based on the R-phase transformation. In the fourth and last section of the article, the performance of selected actuators will be characterized in functional tests, and the results will be compared with the calculated results of the mathematical model.

Keywords actuator, design, heat treatment, R-phase

1. Introduction

Some technical applications in heating technology, like, e.g., thermostatic valves, need temperature-sensitive actuators with small temperature hysteresis, high forces, and good dynamic behavior. The most used actuators in this area are heated expansion elements. They have the advantages such as robustness, relatively high stroke and force. The disadvantages associated with them, however, are temperature hysteresis and slow dynamic behavior (Ref 1). Shape memory alloy (SMA) actuators based on the R-phase transformation are an alternative for expansion elements. The rhombohedral R-phase is an intermediate phase during the transformation from cubic austenite (B2) to monoclinic martensite (B19′). The R-phase transformation (B2 ⇒ R) in NiTi-based alloys has the following advantages (+) and disadvantages (−), compared with the martensitic transformation (B2 ⇒ B19′):

+ small temperature hysteresis of 2-5 °C (Ref 2),
+ high durability up to 500,000 cycles (Ref 3),
− small SMA effect with approximately 0.8% (Ref 4),
− small loadability with approx. 150 MPa (Ref 5).

This article is an invited paper selected from presentations at the International Conference on Shape Memory and Superelastic Technologies 2011, held November 6-9, 2011, in Hong Kong, China, and has been expanded from the original presentation.

K. Lygin, S. Langbein, P. Labenda, and **T. Sadek**, Ruhr-University Bochum, Bochum, Germany. Contact e-mail: lygin@lmk.rub.de.

Skillful design of R-phase actuators, for example, by the use of a helical spring as a form, can minimize the disadvantages of this martensite transformation.

The R-phase transformation forms under certain conditions as follows:

- in Ni-rich binary NiTi alloys—through aging in the temperature range between 350 and 500 °C (Ref 6),
- through cold-working and a subsequent annealing procedure at temperatures between 300 and 550 °C (Ref 7),
- in ternary NiTi-based alloys—through addition of a third element, e.g., Fe (Ref 8), Co, or Al (Ref 4).

In Ni-rich alloys, the presence of precipitates is responsible for the R-phase transformation. The strain fields introduced by precipitates stabilize the R-phase (Ref 9). Depending on the aging temperature and duration, Ni_4Ti_3, Ni_3Ti_2, or Ni_3Ti precipitates are formed in the alloy. Ni_4Ti_3 precipitates are considered the most important for technical applications because they appear at short annealing times and low aging temperatures (Ref 10).

The cold-working process causes formation of the nanocrystalline grain structure, which impedes the nucleation of B19′-phase and promotes the R-Phase transformation because of its lower transformation strain (Ref 11).

However, there are only a very few known actuator applications based on R-phase transformation. Much of the scientific research is focused on the general material behavior in the microstructure (Ref 12, 13) or influences of the thermomechanical heat treatment (Ref 14–16) on the R-phase transformation. The development of R-phase actuators, their production, and validation in functional tests still remain underrepresented in scientific research.

We offer an approach for engineering and validation of SMA actuator elements based on R-phase transformation, the so-called EnVaR. To evaluate this approach, several SMA compression and extension spring actuators will be developed, produced, and validated.

2. Materials and Methods

Commercially available cold-worked binary NiTi materials in the form of wires and springs were investigated in this article. The properties and parameters of the materials are shown in Table 1.

For the activation tests, the wires with a diameter of 0.79 mm were formed to extension springs ($D = 5.9$ mm, $n = 20$). All the wires and springs were heat treated at different temperatures between 300 and 500 °C for durations between 10 and 60 min using an electrical muffle furnace and then quenched in water. Figure 1 shows the winding tools used and the compression and extension SMA springs produced in this study.

A home-constructed activation test rig was used to measure the transformation behavior of the SMA springs. In this test rig, one end of the spring was fixed, while the other end was in a free-floated state and connected to loads between 2 and 8 N. During the activation of the spring by means of electrical current, the transformation temperatures, A_s, A_f, R_{sc}, and R_{fc}, were detected with a thermocouple. The thermocouple was welded onto the surface of the spring. During the experiments, the test rig was positioned in a climatic chamber at temperatures near −20 °C.

A differential scanning calorimeter (TA-Instruments DSC29 20CE) was used to measure the transformation temperatures, A_s, A_p, A_f, R_{sc}, R_{pc}, R_{fc}, M_s, M_p, M_f, R_{sh}, R_{ph}, and R_{fh} (see Fig. 2) with heating and cooling rates of 10 °C/min. The subscripts, "s" means start; "f"—finish; "c"—cooling; "h"—heating; and "p"—peak.

Table 1 Properties of used NiTi wires

Alloy name	Ni-content, wt.%	Ni-content, at.%	Degree of cold forming, %	Wire diameter *d*, mm
S	55.94	50.8	approx. 30	0.79
B	55.66	50.6	approx. 30	0.79
M	55.49	50.4	approx. 30	1.55

3. Research Objective

Actuators based on the R-phase behavior are rarely used in technical applications. One possible reason for this fact is that only a few tools are available, which allow the dimensioning or simulation of the behavior (e.g., dynamic characteristics or fatigue behavior) for SMA-based actuators. Furthermore, most engineers are not familiar with the SMA technology and lack knowledge for designing products based on this new technology.

In order to resolve some of the issues described above, the methodical approach, EnVaR, was developed (see Fig. 3). This

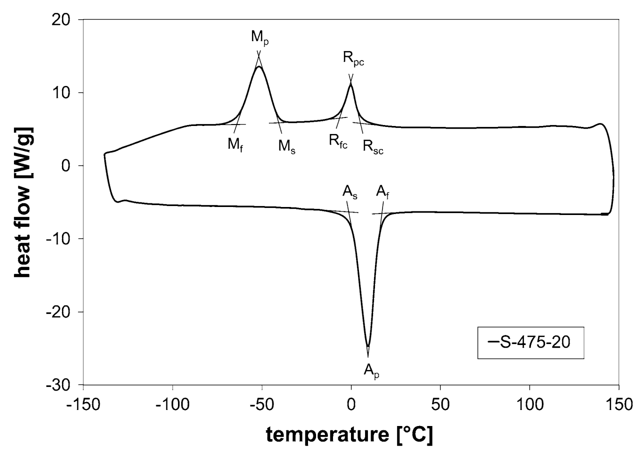

Fig. 2 Representative DSC curve and identification of transformation temperatures

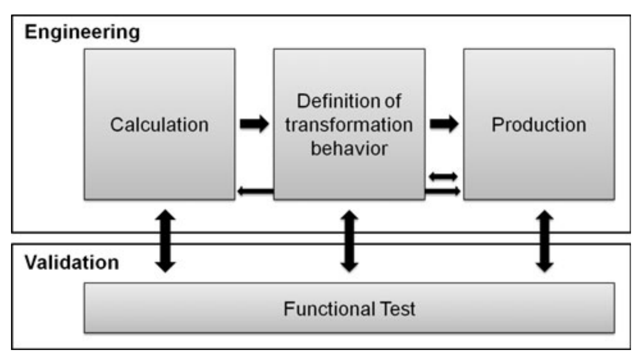

Fig. 3 "EnVaR" approach for development, production, and validation of R-phase actuators

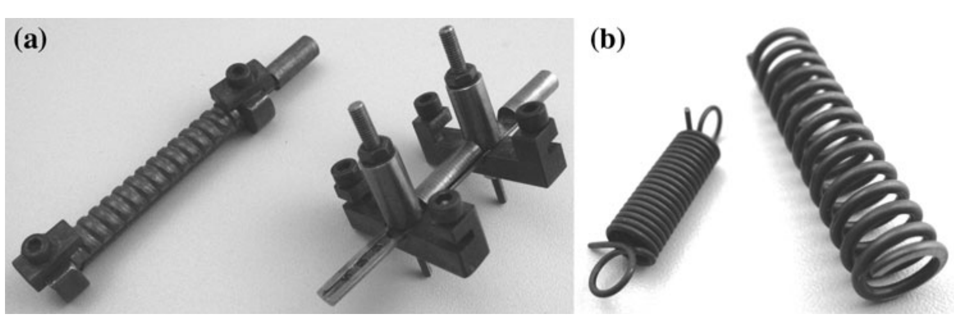

Fig. 1 Winding tools (a) and SMA springs produced (b)

approach consists of an engineering component and a validation component. Regarding the engineering section, a three-part procedural approach is presented, which includes the calculation, definition of transformation behavior, and production of the SMA actuator. Each step is supported by tools (e.g., for the dimensioning) or data (e.g., diagrams which show the distribution of the transformation temperature depending on the Ni-concentration and the selected thermomechanical treatment), which help the designer to use shape memory technology (SMT) to its full extent. All the three steps cannot be regarded on their own individual capacity since they feature multiple interdependencies. The following example illustrates the interdependencies: By means of the calculation tool of the EnVaR approach, a winding ratio of 4 for the SMA spring could be computed. However, the realization of this ratio during production proves quite problematic because of the mechanical properties of the material, which limit the inherent bend radius. This clearly shows the interdependencies of the methodical parts, which need to be considered during a product development.

Regarding the validation part (see bottom of Fig. 3), several methods for a functional assessment are proposed to validate the behavior of the actuator. Hereby, the most important parameters, which need to be examined before the production of the actuator, are defined.

4. Calculation of SMA Actuator

The aim of the first step calculation in the engineering part of the EnVaR approach is the dimensioning of the SMA actuator and the forecast of its stroke/force performance.

The dimensioning of a SMA spring actuator is based on the design rules of conventional springs, e.g., as found in the European Norms (Ref 17). One specific constraint that applies here, in contrast to the conventional springs, is that the shear modulus of a SMA spring is not constant and changes drastically between low- and high-temperature phases. Ohkata and Suzuki (Ref 5) uses this behavior for dimensioning actuator spring with the shape memory effect in his approach. The spring actuators usually work in conjunction with a constant load or a conventional bias steel spring. The load or the steel spring prestresses the SMA spring in the low temperature phase. During the transformation in the high temperature phase, the spring extends because of SM-effect and produces stroke and force. In order to support the designer during this calculation step, the described behavior of the actuator was implemented in a Visual Basic Tool (see Fig. 4).

The dimensioning of a spring actuator is now possible by supplying the requirements of displacement and pulling load as well as some constants. Regarding these constants, the maximum shear stress σ_{max}, the maximum shear strain γ_{max}, the apparent shear moduli G_l and G_h of, respectively, low- and high-temperature phases are necessary. Similar data for the maximum shear strain and maximum stress can be found in the literature (Ref 4, 5). In contrast to this, the information for the shear modulus differs depending on the literature origin (Ref 5, 18). Therefore, the mechanical properties of the material used in the presented study were evaluated through tensile testing (see Fig. 5).

Based on these experiments, the apparent shear modulus was calculated using the various measured curves. The calculated value serves as a basis for the dimensioning tool with respect to the low- and high-temperature phases.

Figure 5 shows the results of the extension experiments of the alloy S (50.8at.%Ni). The apparent shear modulus was determined using Eq 1:

$$G = \frac{F}{s}\frac{8D^3 n}{d^4} \quad \text{(Eq 1)}$$

The term F/s correlates to the ascending slope c of the measured curves for varying temperatures. For the analysis, the curves were linearized. The results of the calculation of the apparent shear modulus are shown in Table 2. Here, it can be seen that the apparent shear modulus between the low- and high-temperature phases varies by about 13.300 N/mm^2 (Fig. 5).

For the evaluation of the quality of the calculations and the measured constants, a spring was dimensioned according to the

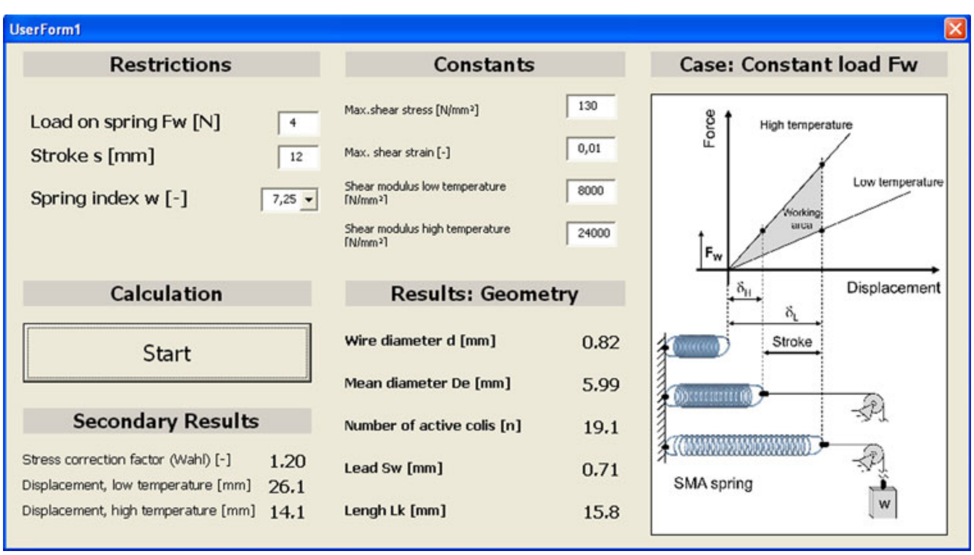

Fig. 4 Calculation tool for R-phase extension spring actuators

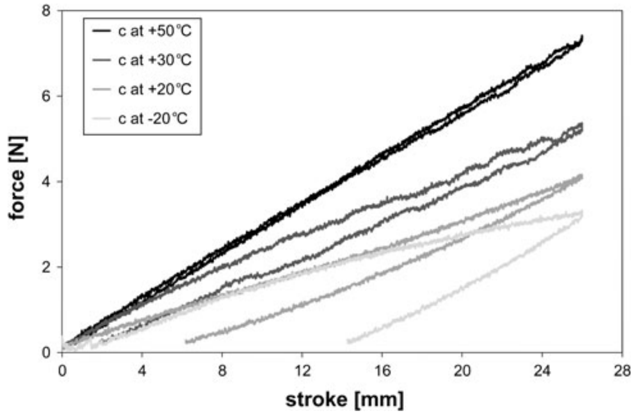

Fig. 5 Force-stroke behavior at different temperatures of alloy S (50.8at.%Ni)

Table 2 Apparent shear modulus at different ambient temperatures

	Ambient temperature, °C			
	−20	**20**	**30**	**50**
Apparent shear modulus G, N/mm^2	10,707	13,855	16,873	24,011

calculated values of the tool. As an evaluation parameter, the thermomechanical behavior of the actuator was chosen. The overall evaluation can be found in the chapter validation.

5. Definition of Transformation Behavior

The engineering-step definition of transformation behavior offers support for the specification of the material and its thermomechanical treatment (Fig. 6). The aim of this engineering step is the prediction of transformation temperatures of the SMA actuator.

The transformation temperatures depend essentially on Ni-concentration, contaminations, degree of cold forming, parameters of heat treatment (especially annealing temperature and time), and quenching. This study specifically focuses on the parameters: Ni-content and annealing temperature.

For technical applications of SMA, the Ni-concentration does mostly vary between 49 and 52at.%Ni (Ref 19). Changing the Ni-concentration by about 0.1at.%Ni leads to a difference in the transformation temperature of up to 10 °C (Ref 10). Regarding these results, the Ni-concentration is a very important and influential parameter for adjusting the phase transformation temperature of an R-phase actuator.

In order to examine the influence of the Ni-concentration on the R-phase transformation, cold-formed SMA samples with different compositions (50.4-50.8at.%Ni) were annealed for 20 min at a temperature of 400 °C. These specifically annealed samples were then examined in the DSC with regard to the peak temperatures of the martensite transformation (see Fig. 7).

The results show that for increasing Ni-concentration, the peak temperatures of the R-phase adjust to lower temperatures. The change of the peak temperature of the R-phase transformation

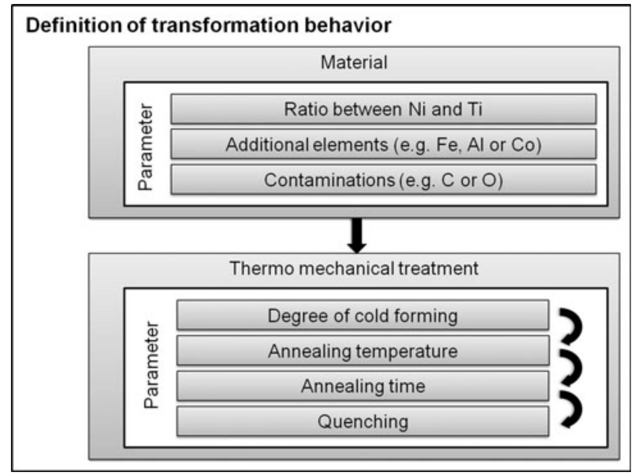

Fig. 6 Content of the engineering step definition of transformation behavior

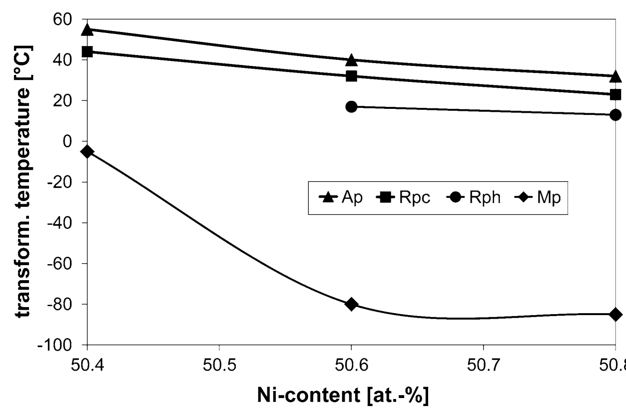

Fig. 7 Transformation temperatures depending on Ni-content at 400 °C annealing temperature and at 20 min annealing time

from 50.4 to 50.8 at.% alloys amounts to approx. 20 °C (R_{pc} decrease from 44 to 23 °C). The martensite peak temperature M_p of the 50.4 at.% alloy can be found at −5 °C. For richer alloy compositions, the temperature decreases even more (from −80 to −85 °C). Technical applications require quite low M_p temperatures, because during a transformation to martensite, the sequence B2 ⇒ R ⇒ B19′ would be passed, resulting in a loss of the lower temperature hysteresis.

When examined with the DSC, both the 50.6 and the 50.8 at.% samples feature an additional martensitic transformation, presumable B19′ ⇒ R, while heating.

The variation of the Ni-concentration is just one possible approach to adjust the transformation temperatures of the R-phase. Another method is based on the variation of the annealing temperature. In this article, the annealing temperature block of 300-500 °C was examined, since this range features the R-phase transformation. As stated before, the precipitates in the applied Ni-rich alloys are responsible for the R-phase transformation. Temperatures below 300 °C did not show the formation of any precipitates. For temperatures > 550 °C, these precipitates tend to dissolve (Ref 7). Figure 8 shows the variation of the heat treatment temperatures of samples with 50.8at.%Ni. It can be seen that the R-phase peak temperature R_{pc} changes from 32 °C (325 °C annealing temperature) to

0 °C (for 475 °C annealing temperature). The austenite peak temperature A_p also decreases with rising annealing temperatures. In contrast, the M_p temperature does increase from −100 to −50 °C for rising annealing temperatures.

The behavior of the R-phase transformation temperature in connection with the annealing temperature as shown in Fig. 8 can also be confirmed with the 50.6 at.% sample (see Fig. 9). The transformation temperatures decrease with increasing heat-treatment temperature. Since these samples contain less Ni, the temperatures are approx. 10 °C higher.

The sample with 50.4at.%Ni shows a slightly different characteristic, since its transformation temperatures do not vary and its mean value is located at an approximately constant 48 °C.

6. Production Process of the SMA Actuator

The aim of the engineering-step production is the definition of a process, selection of process parameters, and production of the SMA actuator.

Regarding the Ni-rich alloys that are featured in this article, it could be possible to conduct a reference production process

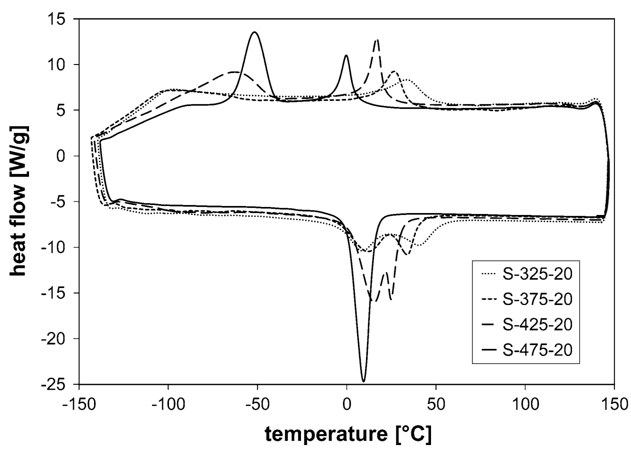

Fig. 8 Transformation temperatures depending on annealing temperature (duration 20 min) in alloy S (50.8at.%Ni)

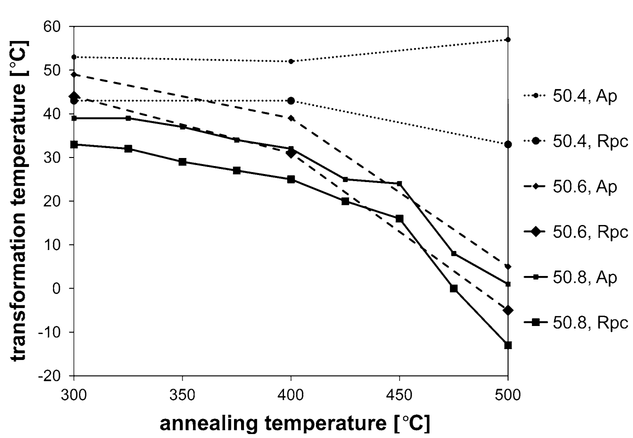

Fig. 9 Transformation temperature depending on annealing temperature at different Ni-contents

by using the schematics shown in Fig. 10. Alternative production processes that include, e.g., hot forming are not considered in this study and need further research.

The production process consists of the four steps: cold drawing, coiling, annealing, and quenching. Each process phase features different process parameters that can be varied in limited intervals. Furthermore, the shown approach offers a trend that explains which effect a variation of a process parameter does have and therefore helps the designer to decide on his/her actions. As an example, it is possible to vary the process parameter "annealing temperature" between 300 and 550 °C. The designer of this approach will then be notified that the corresponding influence of the rising annealing temperature is a decreasing transformation temperature. The information for these references for the designers originate from the own experience of the authors, other literature studies, or from results of conducted experiments.

7. Functional Test of the SMA Actuator

The aim of the validation step functional test is to check the functional properties of the produced SMA actuators and a comparison with the results of actuator engineering from the EnVaR methodology. For the validation of the functional properties, a pull spring was produced (compare Fig. 1) using the following specific geometry (d = 0.79 mm, D = 5.9 mm, and n = 20) and annealing parameters (T_A = 400 °C and t_A = 20 min). The spring was then activated with a load of 4 N, and its displacement characteristics were determined (see Fig. 11).

The displacement characteristics of the aforementioned spring was measured and then compared to the results of the calculation of the EnVaR methodology. Table 3 shows the results of the comparison.

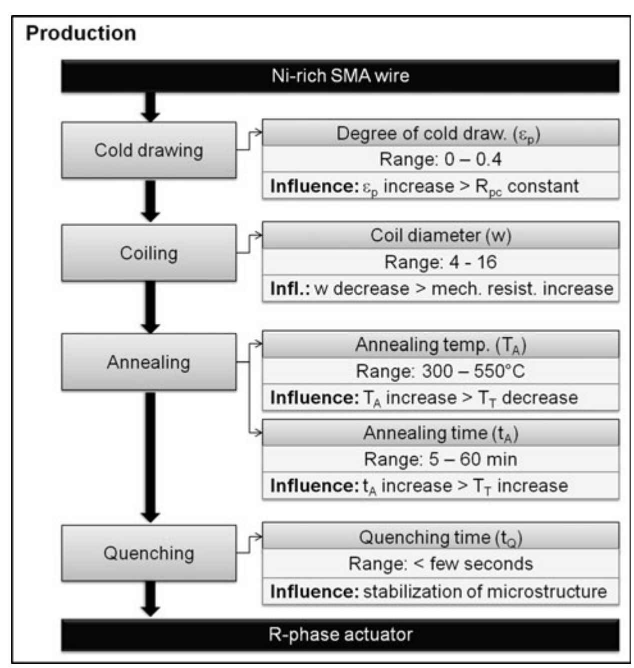

Fig. 10 Content of the engineering step production

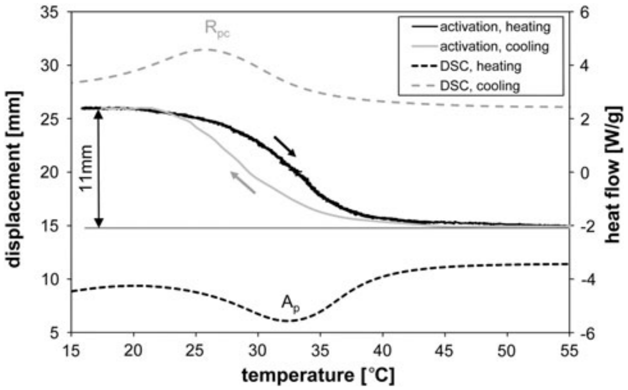

Fig. 11 Comparison between DSC and activation test of a SMA spring with 50.8at.%Ni

Table 3 Comparison between calculation and activation test at 4 N load

Parameter	Calculation, mm	Test, mm	Deviation, mm
Displacement at low temperature	26.1	26.0	+0.1
Displacement at high temperature	14.1	14.8	−0.7
Stroke	12.0	11.3	−0.7

The results of the comparison show that only minor differences between the calculation and the functional tests of the spring can be identified. These differences might also result from external influences like the measuring system and its inherent friction. Furthermore, it was not possible to produce the spring with the exact calculated process parameters. In addition, slight differences between the applied and simulated wire- and spring-diameters might add to the minor deviations. An additional test examined the transformation behavior of the spring. Therefore, a comparison of the transformation temperatures measured by a DSC in an activation test was conducted. The results can also be found in Fig. 11. It is shown that the transformation behavior of the DSC measurement corresponds to the transformation behavior of the activation curve.

8. Summary and Conclusion

In this article, a methodology called EnVaR for the developing, producing, and validating of R-phase springs is presented. Excerpts of the methodology, e.g., the calculation of definition of the transformation behavior are explained in detail, and the corresponding tools or experiments to support the designer were described and explained. The methodology itself was verified by the demonstration of a working spring actuator. It has been shown that the EnVaR methodology is helpful to the designer in dimensioning the R-phase actuators and providing useful information during the different process steps. Furthermore, the methodology by means of its calculation tools is able to predict the behavior of R-phase actuators in close approximation with regard to their displacement characteristics, pulling load, and the corresponding transformation temperatures.

Acknowledgments

The authors acknowledge the funding for this research under project T4 of the Collaborative Research Center SFB459 (shape memory technology) funded by the Deutsche Forschungsgemeinschaft (DFG), North Rhine-Westphalia and the Ruhr University Bochum.

References

1. R. Isermann, *Mechatronic Systems*, 2nd ed., Springer, Berlin, 2009, p 504 (in German)
2. Z. Zhoua, G. Fana, J. Zhang, X. Ding, X. Ren, J. Suna, and K. Otsuka, Understanding of Multi-Stage R-Phase Transformation in Aged Ni-Rich Ti-Ni Shape Memory Alloys, *Mater. Sci. Eng. A*, 2006, **438–440**, p 602–607
3. P. Sittner, M. Landa, P. Lukas, and V. Novak, R-Phase Transformation Phenomena in Thermomechanically Loaded NiTi Polycrystals, *Mech. Mater.*, 2006, **38**, p 475–492
4. T. Saburi, Ti-Ni Shape Memory Alloys, *Shape Memory Materials*, K. Otsuka and C.M. Wayman, Ed., Cambridge University Press, Cambridge, 1998, p 49–96
5. I. Ohkata and Y. Suzuki, The Design of SMA Actuators and Their Applications, *Shape Memory Materials*, K. Otsuka and C.M. Wayman, Ed., Cambridge University Press, Cambridge, 1998, p 240–266
6. H. Sadiq, M.B. Wong, R. Al-Mahaidi, and X.L. Zhao, The Effects of Heat Treatment on the Recovery Stresses of Shape Memory Alloys, *Smart Mater. Struct.*, 2010, **19**, p 35021–35027
7. D. Treppman, *Thermomechanical Treatment of NiTi*, VDI-Verlag, Düsseldorf, 1997 (in German)
8. V.B. Krishnan, R.M. Manjeri, B. Clausen, D.W. Brown, and R. Vaidyanathan, Analysis of Neutron Diffraction Spectra Acquired In Situ During Mechanical Loading of Shape Memory NiTiFe at Low Temperatures, *Mater. Sci. Eng. A*, 2008, **481–482**, p 3–10
9. X. Ren, N. Miura, J. Zhang, K. Otsuka, K. Tanaka, M. Koiwa, T. Suzuki, Y. Chumlykov, and M. Asai, A Comparative Study of Elastic Constants of Ti-Ni-Based Alloys Prior to Martensitic Transformation, *Mater. Sci. Eng. A*, 2001, **312**, p 196–200
10. J. Frenzel, E.P. George, A. Dlouhy, Ch. Somsen, M.F.-X. Wagner, and G. Eggeler, Influence of Ni on Martensitic Phase Transformations in NiTi Shape Memory Alloys, *Acta Mater.*, 2010, **58**, p 3444–3458
11. J. Frenzel, J.A. Burow, E.J. Payton, S. Rezanka, and G. Eggeler, Improvement of NiTi Shape Memory Actuator Performance Through Ultra-Fine Grained and Nanocrystalline Microstructures, *Adv. Eng. Mater.*, 2010, **13**(4), p 256–268
12. W. Cai, Y. Murakami, and K. Otsuka, Study of R-Phase Transformation in a Ti-50.7at%Ni Alloy by In-Situ Transmission Electron Microscopy Observations, *Mater. Sci. Eng. A*, 1999, **273–275**, p 186–189
13. X. Zhang and H. Sehitoglu, Crystallography of the B2 $\rightarrow$ R $\rightarrow$ B19′ Phase Transformations in NiTi, *Mater. Sci. Eng. A*, 2004, **374**, p 292–302
14. A.S. Paula, K.K. Mahesha, C.M.L. dos Santos, F.M. Braz Fernandes, and C.S. da Costa Viana, Thermomechanical Behavior of Ti-Rich NiTi Shape Memory Alloys, *Mater. Sci. Eng. A*, 2008, **481–482**, p 146–150
15. T. Todoroki and H. Tamura, Effect of Heat Treatment After Cold Working on the Phase Transformation in TiNi Alloy, *Trans. Jpn. Inst. Met.*, 1987, **28**(2), p 83–94
16. D.A. Miller and D.C. Lagoudas, Influence of Cold Work and Heat Treatment on the Shape Memory Effect and Plastic Strain Development of NiTi, *Mater. Sci. Eng. A*, 2001, **308**, p 161–175
17. European Norm EN 13906-2, *Cylindrical Helical Springs Made from Round Wire and Bar—Calculation and Design—Part 2: Extension Springs*, Beuth Verlag, Berlin, 2002
18. T.W. Duerig, K.N. Melton, D. Stöckel, and C.M. Wayman, *Engineering Aspects of Shape Memory Alloys*, Butterworth-Heinemann Ltd., London, 1990
19. M. Mertmann, *NiTi-Formgedächtnislegierungen für Aktoren der Greiftechnik*, VDI, Verlag, Düsseldorf, 1997 (in German)